Tachycardia-induced silencing of subcellular Ca^{2+} signaling in atrial myocytes

Maura Greiser,[1,2] Benoît-Gilles Kerfant,[1] George S.B. Williams,[2] Niels Voigt,[3] Erik Harks,[1] Katharine M. Dibb,[4] Anne Giese,[1] Janos Meszaros,[1] Sander Verheule,[1] Ursula Ravens,[5] Maurits A. Allessie,[1] James S. Gammie,[6] Jolanda van der Velden,[7] W. Jonathan Lederer,[2] Dobromir Dobrev,[3] and Ulrich Schotten[1]

[1]Department of Physiology, Maastricht University, Maastricht, the Netherlands. [2]Center for Biomedical Engineering and Technology, Laboratory of Molecular Cardiology, and Department of Physiology, University of Maryland School of Medicine, Baltimore, Maryland, USA. [3]Institute of Pharmacology, Faculty of Medicine, University Duisburg-Essen, Essen, Germany. [4]Unit of Cardiac Physiology, Manchester Academic Health Sciences Centre, Manchester, United Kingdom. [5]Department of Pharmacology and Toxicology, Dresden University of Technology, Dresden, Germany. [6]Division of Cardiac Surgery, University of Maryland Medical Center, Baltimore, Maryland, USA. [7]Laboratory for Physiology, VU University Medical Center, Amsterdam, the Netherlands.

Atrial fibrillation (AF) is characterized by sustained high atrial activation rates and arrhythmogenic cellular Ca^{2+} signaling instability; however, it is not clear how a high atrial rate and Ca^{2+} instability may be related. Here, we characterized subcellular Ca^{2+} signaling after 5 days of high atrial rates in a rabbit model. While some changes were similar to those in persistent AF, we identified a distinct pattern of stabilized subcellular Ca^{2+} signaling. Ca^{2+} sparks, arrhythmogenic Ca^{2+} waves, sarcoplasmic reticulum (SR) Ca^{2+} leak, and SR Ca^{2+} content were largely unaltered. Based on computational analysis, these findings were consistent with a higher Ca^{2+} leak due to PKA-dependent phosphorylation of SR Ca^{2+} channels (RyR2s), fewer RyR2s, and smaller RyR2 clusters in the SR. We determined that less Ca^{2+} release per $[Ca^{2+}]_i$ transient, increased Ca^{2+} buffering strength, shortened action potentials, and reduced L-type Ca^{2+} current contribute to a stunning reduction of intracellular Na^+ concentration following rapid atrial pacing. In both patients with AF and in our rabbit model, this silencing led to failed propagation of the $[Ca^{2+}]_i$ signal to the myocyte center. We conclude that sustained high atrial rates alone silence Ca^{2+} signaling and do not produce Ca^{2+} signaling instability, consistent with an adaptive molecular and cellular response to atrial tachycardia.

Introduction

With the onset of atrial fibrillation (AF), atrial activation rates increase 5- to 7-fold (1). Initially, this causes intracellular Ca^{2+} overload (2). Subsequent adaptation to the high rate (atrial remodeling) leads to a "self-correction," with the transient high intracellular Ca^{2+} returning to near-normal levels (3). However, while intracellular Ca^{2+} levels are normalizing, there is also evidence that unstable intracellular Ca^{2+} signaling develops in AF (4). This Ca^{2+} signaling instability has been suggested to contribute to atrial arrhythmogenicity and maintenance of AF (5). It is unclear whether unstable Ca^{2+} signaling develops as a consequence of the rapid rate (i.e., during initial episodes of paroxysmal AF) or whether it is caused by underlying heart disease. Likewise, the contribution of Ca^{2+} signaling instability to the initiation and perpetuation of AF is unknown. Upregulation of Ca^{2+}/calmodulin-dependent kinase II (CaMKII) and protein kinase A–dependent (PKA-dependent) phosphorylation has been shown to produce increased Ca^{2+} sensitivity of cardiac Ca^{2+} release channels (ryanodine receptors, RyR2s), leading to higher Ca^{2+} spark and Ca^{2+} wave frequencies (6, 7). Indeed, evidence for increased CaMKII activity is commonly found in atrial tissue from patients with persistent AF (5, 8). High CaMKII levels in AF have been attributed to a high atrial activation rate (7), because an increased frequency of intracellular Ca^{2+} oscillations has been shown to produce sustained increases in CaMKII activity (9). Thus, how atrial cells from intact animals respond to sustained high atrial rates with respect to their Ca^{2+} signaling is critical to an investigation of the causes of AF. Importantly, many AF patients have substantial concomitant cardiovascular disease (e.g., hypertension, valvular disease, heart failure) (10), which can independently produce arrhythmogenic unstable Ca^{2+} signaling (11). It is therefore difficult to separate the contributions of each disease entity to the unstable intracellular Ca^{2+} signaling in AF. While a rapid atrial rate is a central element in the sequence of events that converts a patient from sinus rhythm to one with paroxysmal and persistent AF, how the rapidity of the atrial rate itself contributes to this process is unknown.

In the present study, we have characterized the effects of a short-term, sustained high atrial activation rate alone (rapid atrial pacing [RAP], 10 Hz, 5 days) on intracellular Ca^{2+} signaling in a rabbit model. We have identified an array of dramatic and important changes in molecular signaling pathways that make profound contributions to atrial Ca^{2+} regulation. The surprising finding is that rapid atrial activation appears to produce an antiarrhythmic array of responses that we call "Ca^{2+} signaling silencing." As part of this response, CaMKII expression levels were unchanged, and CaMKII-mediated RyR2 phosphorylation was reduced. Surprisingly, $[Na^+]_i$ was also reduced. In addition, we show that a key element of Ca^{2+} signaling silencing, the failure of the intracellu-

▶ Related Commentary: p. 4684

Conflict of interest: The authors have declared that no conflict of interest exists.
Submitted: March 23, 2013; **Accepted:** August 28, 2014.
Reference information: *J Clin Invest*. 2014;124(11):4759–4772. doi:10.1172/JCI70102.

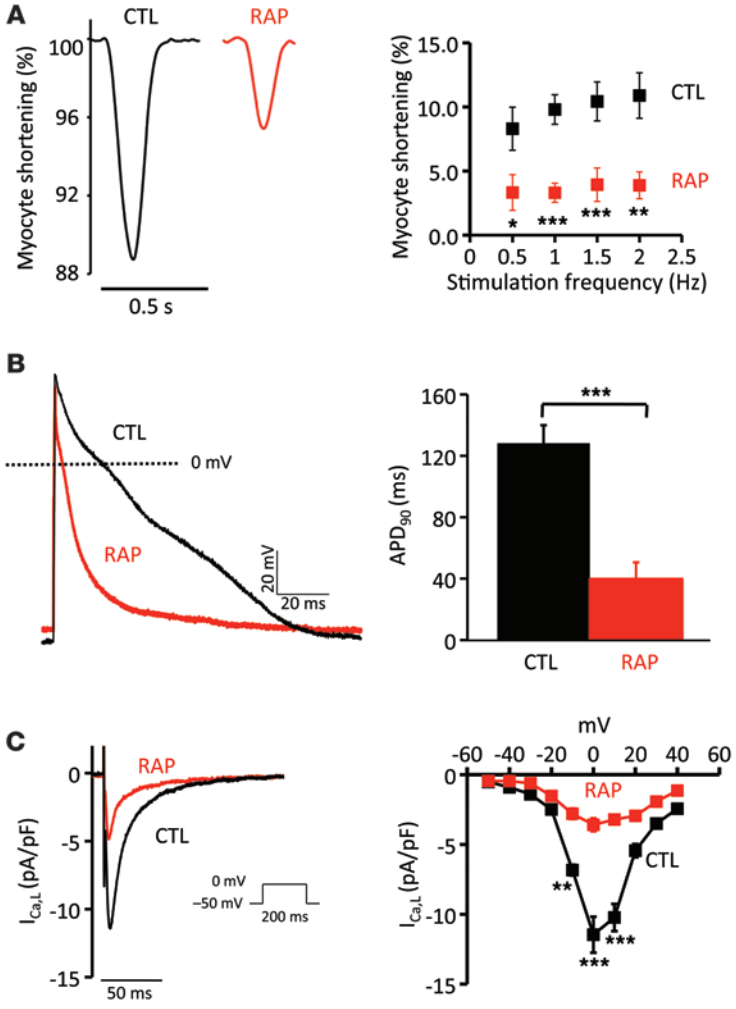

Figure 1. Contractile and electrical remodeling after RAP. (**A**) Fractional myocyte shortening (CTL: *n* = 18 cells, 6 animals; RAP: *n* = 21 cells, 5 animals). (**B**) Cellular AP and APD at 2 Hz (CTL: *n* = 15 cells, 7 animals; RAP: *n* = 12 cells, 6 animals). (**C**) Left panel: Original recordings of $I_{Ca,L}$ in a CTL and RAP cell. Right panel: Current-voltage relation (CTL: *n* = 19 cells, 6 animals; RAP: *n* = 17 cells, 5 animals).*$P < 0.05$; **$P < 0.01$; ***$P < 0.001$.

lar Ca^{2+} wave, also occurs in persistent human AF. Here, we have investigated the changes quantitatively and discuss the role that they may play in response to AF and in the development of diverse pathophysiologic consequences.

Results

RAP model

To examine the effect of sustained, short-term high atrial activation rates in the absence of confounding disease, we established an in vivo RAP rabbit model (see Methods below and Supplemental Figure 1; supplemental material available online with this article; doi:10.1172/JCI70102DS1). The model imposed 5 days of RAP at 10 Hz followed by measurement of atrial effective refractory periods (AERPs). After 5 days of RAP, the AERPs in the intact animals were significantly shortened compared with those in the sham-operated animals (Supplemental Figure 1), which served as controls (CTLs).

Contractile and electrical remodeling in RAP rabbits

We found that myocyte fractional shortening was reduced over a range of stimulation frequencies in cells isolated from RAP animals (RAP cells). The positive frequency-shortening relation we observed in CTL myocytes was lost in the RAP cells (Figure 1A).

Action potential duration (APD) was significantly shortened in RAP cells (Figure 1B). Peak L-type Ca^{2+} current ($I_{Ca,L}$) density was significantly reduced in RAP cells (Figure 1C).

Transverse tubules

Di-8-ANEPPS staining revealed only nominal transverse tubule (TT) density in CTL and RAP rabbit left atrial myocytes (Supplemental Figure 2A). We found that TT distribution in human left atrial myocytes was similarly sparse in CTL left atrial myocytes isolated from patients in sinus rhythm and was unchanged in myocytes from AF patients (Supplemental Figure 2B). TT density in CTL mouse left atrial myocytes, however, was 8.1%, which is higher than in rabbit or human left atrial myocytes and similar to TT density in larger mammals (i.e., sheep and dog atrial myocytes; Supplemental Figure 2C and refs. 12, 13).

Effect of a rapid rate on intracellular Ca^{2+} release

Whole-cell Ca^{2+} transients. During 2 Hz field stimulation, the steady-state whole-cell $[Ca^{2+}]_i$ transient (CaT) amplitude was significantly lower in RAP cells compared with that in CTL cells (Supplemental Figure 3, A and B). We found that RAP CaTs displayed a faster upstroke (time to peak, 90%) and decay (time to baseline, 50%) compared with CTL cells (Supplemental Figure 3C). Importantly, diastolic $[Ca^{2+}]_i$ was unchanged in RAP cells compared with that detected in CTL cells (Supplemental Figure 3D).

Failure of regenerative Ca^{2+} wave propagation after RAP. In intact CTL myocytes, transverse confocal linescan images of subsarcolemmal (ss) and central-cellular (cc) CaTs recorded during steady-state field stimulation (2 Hz) showed similar CaT amplitudes (Figure 2A). However, RAP cells had a significantly reduced cc CaT amplitude compared with that of the ss CaT, indicating a failure of the regenerative centripetal Ca^{2+} wave propagation (Figure 2, B and C). Surprisingly, we found that the ss CaT amplitude was not reduced in RAP cells compared with that seen in CTL cells, despite a significantly reduced L-type Ca^{2+} current density in the RAP cells.

Post-rest potentiation experiments showed a restoration of the intracellular Ca^{2+} release wave after 20 s of rest in RAP cells, suggesting that the failure of Ca^{2+} wave propagation was functional rather than structural (Supplemental Figure 4).

Reduced $I_{Ca,L}$ does not cause failure of regenerative Ca^{2+} wave propagation

$I_{Ca,L}$ reduction is a hallmark of AF-induced remodeling (14, 15) and is thought to play a central role in the adaptive alteration of Ca^{2+} signaling in AF (4). In order to characterize the effect of $I_{Ca,L}$ reduction alone on subcellular $[Ca^{2+}]_i$ signaling, we treated CTL cells with the L-type Ca^{2+} channel (DHPR) antagonist nitrendipine (0.3 μmol/l). Spatially resolved Ca^{2+} imaging revealed similar reductions in ss and

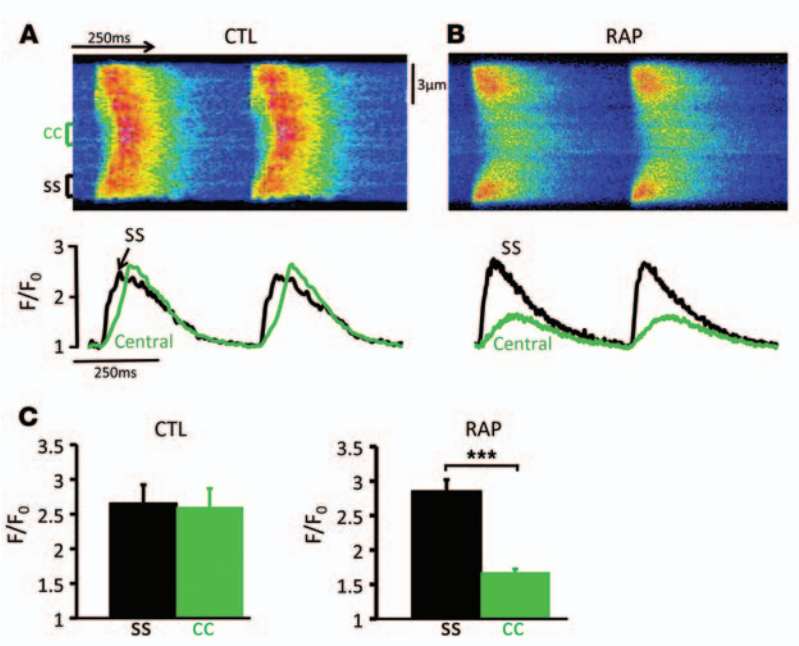

Figure 2. Failure of centripetal Ca^{2+} wave propagation after RAP. (**A**) Transverse confocal linescan and derived local CaTs from a CTL cell showing similar amplitudes of ss and cc CaTs. (**B**) Transverse confocal linescan and derived local CaTs from an RAP cell showing the significantly blunted cc CaT. (**C**) Reduced cc but preserved ss CaT amplitude in RAP cells at 2 Hz (CTL: n = 28 cells, 6 animals; RAP: n = 26 cells, 6 animals). ***$P < 0.001$. F, fluorescence intensity; F_0, baseline fluorescence intensity.

cc CaT amplitudes in nitrendipine-treated CTL cells (Figure 3, A and B). Surprisingly, these results demonstrated a different pattern of subcellular Ca^{2+} signaling than we observed in RAP cells, where the ss CaT amplitude was unaltered. Whole-cell CaT amplitudes in nitrendipine-treated CTL cells were reduced to a degree similar to those seen in RAP cells in the absence of nitrendipine (Figure 3, C and D). However, the altered CaT kinetics found in RAP cells were not reproduced by the nitrendipine-induced $I_{Ca,L}$ reduction in CTL cells. CaT decay and time to peak in nitrendipine-treated cells did not differ from untreated CTL myocytes (Figure 3, C and D). Approximation of the sarcoplasmic reticulum (SR) Ca^{2+} load from the amplitude of the caffeine-induced CaT showed that the SR Ca^{2+} appeared not to be depleted in nitrendipine-treated CTL cells compared with that in the untreated CTL cells, showing that a reduction of $I_{Ca,L}$ does not lead to Ca^{2+} depletion in the SR of atrial cells (0.55 ± 0.06 $\Delta F_{340}/F_{380}$ for treated CTL cells vs. 0.61 ± 0.07 $\Delta F_{340}/F_{380}$ for CTL cells; n = 12 cells, $P < 0.05$). Prompted by these results, we performed more quantitative measurements of SR Ca^{2+} content in CTL and RAP cells (see below).

The first derivative of ss CaTs can be used as an approximation for ss SR Ca^{2+} release fluxes (16). As expected, treatment of CTL cells with nitrendipine significantly reduced ss SR Ca^{2+} release fluxes due to the reduced ss trigger Ca^{2+} (Supplemental Figure 5). Interestingly, in RAP cells, the SR Ca^{2+} release fluxes were not changed compared with those of CTL cells, although $I_{Ca,L}$ in the RAP cells was significantly reduced. However, in the nitrendipine-treated CTL cells, the reduced $I_{Ca,L}$ was associated with a reduced ss $[Ca^{2+}]_i$ transient. Thus, in RAP cells, excitation-contraction (EC) coupling appeared to be more efficient than in CTL cells, since we observed an identical ss $[Ca^{2+}]_i$ transient with a much smaller $I_{Ca,L}$. This may reflect the hyperphosphorylation of RyR2 at the PKA site (Ser2808) and the resulting purported increase in $[Ca^{2+}]_i$ sensitivity (see below). Nevertheless, the absence of robust propagation of Ca^{2+}-induced Ca^{2+} release (CICR) in RAP cells leads to a small and delayed cc $[Ca^{2+}]_i$ transient, and this suggests that CICR is reduced in RAP cells (see discussion of buffering below).

Thus, while leading to a similar reduction in whole-cell CaT amplitude, $I_{Ca,L}$ reduction in CTL cells does not mimic subcellular Ca^{2+} signaling in RAP cells. The reduction of the whole-cell CaT in RAP cells and nitrendipine-treated CTL cells in response to reduced Ca^{2+} entry plays a role in the preservation of the SR Ca^{2+} load (17).

A sustained rapid rate induces upregulation of the Na^+-Ca^{2+} exchange function but leaves the SR Ca^{2+} load unchanged

Quantitative SR Ca^{2+} content experiments (see Supplemental Methods) revealed that the I_{NCX} magnitude was greater in RAP cells than in CTL cells at any given $[Ca^{2+}]_i$ (Figure 4C). Since NCX protein expression was unchanged (Supplemental Figure 6A), these data suggest that NCX "upregulation" is functional rather than being based on increased protein expression. The possible underlying mechanisms are presented in the Discussion below.

We further evaluated the non-SR Ca^{2+} ATPase and non-NCX Ca^{2+} extrusion mechanisms (i.e., plasma membrane Ca^{2+} ATPAse; see Supplemental Methods). The rate of non-NCX–mediated Ca^{2+} extrusion (k_{slow}) was unchanged between CTL and RAP cells (Supplemental Figure 7).

We found that the integrated I_{NCX} measured in voltage-clamped atrial myocytes during fast application of 10 mmol/l caffeine did not differ between RAP and CTL cells (Figure 4, A and B), showing that the total SR Ca^{2+} load was unchanged in RAP cells when compared with that in CTL cells. Additionally, confocal imaging revealed that estimates of the domain-specific SR Ca^{2+} load, which are derived from the amplitude of the caffeine-induced CaT, were similar in the center of the cell and near the sarcolemmal membrane (Figure 4D).

Sustained rapid rate decreases $[Na]_i$

$[Na]_i$ is an important regulator of intracellular Ca^{2+} homeostasis and provides insight into NCX activation during RAP. Here, we provide the first measurements of $[Na]_i$ in viable atrial myocytes (Figure 5). Resting $[Na]_i$ in CTL cells was 6.86 ± 0.36 mmol/l. We observed that $[Na]_i$ increased during field stimulation (Fig-

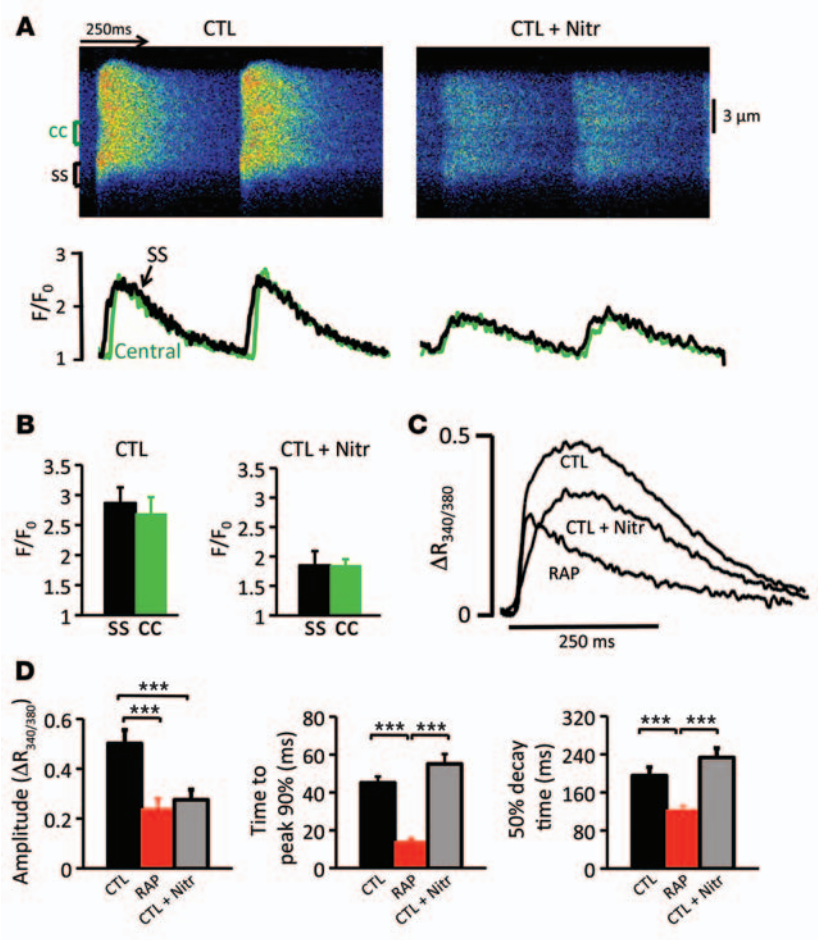

Figure 3. Role of $I_{Ca,L}$ reduction. (**A**) Confocal linescan and derived local CaTs in a CTL myocyte before (left panel) and after (right panel) treatment with the Ca^{2+} channel antagonist nitrendipine (Nitr) (0.3 µmol/l). (**B**) Regional CaT amplitudes at baseline and after application of nitrendipine (n = 15 cells, 4 animals). (**C**) Averaged (n = 20) recordings of whole-cell CaT in CTL cells, CTL cells treated with nitrendipine, and RAP cells. (**D**) Whole-cell CaT amplitude, time to peak, and decay time (CTL and CTL plus nitrendipine: n = 14 cells, 4 animals; RAP: n = 22 cells, 5 animals). ***$P < 0.001$.

ure 5D). Surprisingly, we found that resting $[Na]_i$ was substantially lower in RAP cells (4.02 ± 0.49 mmol/l). Importantly, $[Na]_i$ increased to a similar degree in CTL and RAP cells during field stimulation (Figure 5, C and D). Nevertheless, we found that the amount of absolute $[Na]_i$ in RAP cells was substantially lower at all stimulation rates (Figure 5C). In search of an explanation for the reduced $[Na^+]_i$ in RAP cells, we considered $I_{Ca,L}$. $I_{Ca,L}$ is significantly reduced in RAP cells. Together with the shortening of the APD, this leads to an even more pronounced reduction of Ca^{2+} entry into RAP cells. This results in markedly reduced Na^+ entry via the NCX when sarcolemmal Ca^{2+} is in pump-leak balance. For example, during 1-Hz stimulation, 4 times as much Na^+ enters through the NCX than through voltage-gated Na^+ channels (18). Despa et al. reported that, at rest, 100% more Na^+ entered through the NCX than through Na^+ channels in rabbit myocytes (18). The substantial reduction of Ca^{2+} entry through $I_{Ca,L}$ and Ca^{2+} extrusion (via the NCX) and the coupled reduction in Na^+ entry into RAP cells are likely the main mechanisms underlying the low $[Na^+]$ in these cells. Nevertheless, protein expression levels of sarcolemmal Na^+/K^+ ATPase (NKA) were unchanged between RAP and CTL cells (Figure 5E). Furthermore, phosphorylation of phospholemman (PLM), the regulatory protein of NKA, was reduced at Ser63 and Ser68 (Figure 5F), suggesting reduced NKA function (19, 20). Taken together, it is clear that further investigation of Na^+ dynamics in atrial cells under these conditions and in health and disease is needed.

Sustained rapid rate increases the fast $[Ca^{2+}]_i$ buffering strength

Atrial myocytes with sparse TTs rely on Ca^{2+} diffusion between neighboring RyR2 clusters to activate regenerative Ca^{2+} release from the periphery to the core of the myocyte (21, 22). Changes in the fast Ca^{2+} buffering strength, which is made up of different Ca^{2+}-binding components (e.g., myofilaments and calmodulin), will likely affect the centripetal regenerative $[Ca^{2+}]_i$ release wave in atrial cells without TTs (23). In order to test this hypothesis, we increased the total fast Ca^{2+} buffering strength of CTL myocytes by the addition of the fast Ca^{2+} chelator BAPTA (1 µmol/l). Confocal linescans in these cells revealed an unaltered ss CaT amplitude but a significantly reduced cc CaT amplitude (Figure 6, A and B). Loading estimates (see Supplemental Methods) showed an expected intracellular BAPTA concentration of 110 µmol/l. These results show that increases in fast Ca^{2+} buffering strength induce failure of the regenerative centripetal Ca^{2+} wave propagation.

We assessed intracellular Ca^{2+} buffering strength using a modification of the protocol described by Trafford (24) (see Supplemental Methods). As seen in Figure 6C, more total Ca^{2+} was needed to achieve the same level of free Ca^{2+} in RAP cells compared with CTL cells, showing that more Ca^{2+} is bound to Ca^{2+} buffers in RAP.

Western blot analysis revealed no changes in troponin C (TnC) or troponin I (TnI) protein expression levels (Figure 7, A, B, and E). However, TnI phosphorylation at Ser23/24, a dominant PKA phosphorylation site (25), was significantly reduced in RAP tissue (Figure 7, A and C). This increases TnC Ca^{2+} binding and thus myofilament Ca^{2+} sensitivity (26), resulting in higher intracellular Ca^{2+} buffering strength. Because BAPTA is a mobile Ca^{2+} buffer, we wanted to better evaluate the effect of increases in "stationary" Ca^{2+} buffering (e.g., by the myofilaments) on intracellular Ca^{2+} wave propagation. As a proof of principle, we treated CTL cells with the Ca^{2+} sensitizer EMD 57033, which is known to significantly increase intracellular Ca^{2+} buffering (27). After treatment (30 minutes) with 3 µmol/l, EMD ss CaT amplitude was unaltered, but the core CaT amplitude was significantly reduced (Figure 6D). While the effect of EMD was not as pronounced as that of BAPTA, the results confirm that increased myofilament Ca^{2+} sensitivity can significantly impair the propagation of the centripetal intracellular Ca^{2+} wave.

Calmodulin protein expression was also significantly increased in RAP (Figure 7D), which further contributed to increased

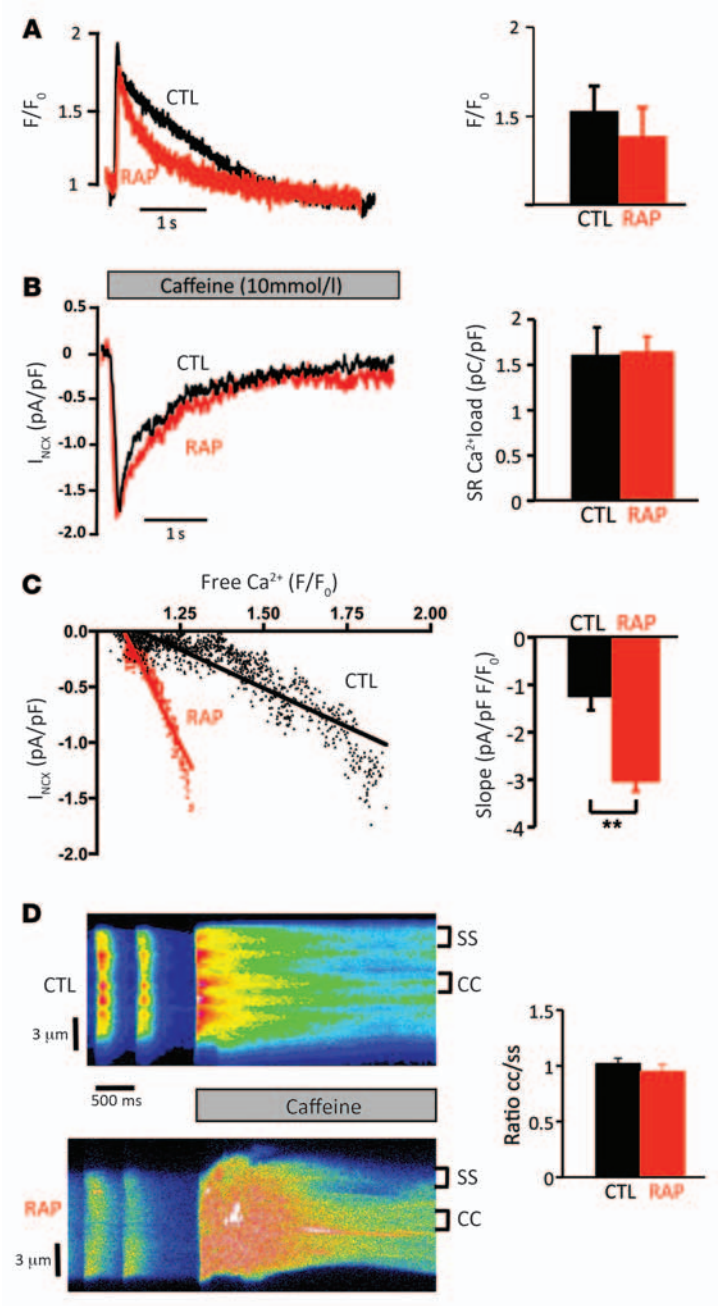

Figure 4. Upregulation of NCX and unchanged SR Ca^{2+} content. (**A**) Left panel: Original recordings of whole-cell CaTs (whole-cell epifluorescence, fluo-3) during caffeine application (10 mmol/l). Right panel: Caffeine-induced CaT amplitude (CTL: n = 22 cells, 5 animals; RAP: n = 16 cells, 5 animals). (**B**) SR Ca^{2+} content: Original recordings of I_{NCX} during caffeine application (10 mmol/l) and SR Ca^{2+} content based on integrated I_{NCX} (CTL: n = 18 cells, 4 animals; RAP: n = 16 cells, 5 animals). (**C**) Example of linear (slow) phase of I_{Ncx} free $[Ca^{2+}]_i$ plot obtained during simultaneous measurement of I_{NCX} and $[Ca^{2+}]_i$ (whole-cell epifluorescence, fluo-3) during fast application of caffeine (10 mmol/l) in voltage-clamped atrial myocytes (CTL: n = 14 cells, 4 animals; RAP: n = 13 cells, 5 animals). (**D**) Left panels: Transverse confocal linescans during caffeine application depicting domain-specific SR Ca^{2+} load in a CTL cell and an RAP cell. (CTL: n = 15 cells, 4 animals; RAP: n = 13 cells, 4 animals). Right panel: Ratio of cc/ss caffeine-induced CaT amplitudes as an approximation of domain-specific SR Ca^{2+} content. $^{**}P < 0.01$.

Ca^{2+} buffering in RAP. We found that myosin-binding protein C (MyBP-C) expression and phosphorylation levels were unchanged in RAP (Supplemental Figure 6B).

Role of SR Ca^{2+} ATPAse

The rate of decline of the $[Ca^{2+}]_i$ transient in the ss compartment is a complex mix of Ca^{2+} extrusion by the sarcolemmal NCX, Ca^{2+} uptake into the ss SR by the ss SR Ca^{2+} ATPAse (Serca2a), Ca^{2+} binding to diverse buffers (as discussed above), and Ca^{2+} diffusion into areas of the cell with lower $[Ca^{2+}]_i$. A consequence of the small cc CaT in RAP, combined with the rapid NCX extrusion and increased cytosolic buffering, is the more rapid decay of the ss CaT in these cells than in CTL cells (Supplemental Figure 8E). Simple computational modeling suggests that the rapid decay of the ss CaT is consistent with these influences and is not due to an enhanced rate of Serca2a activity. Indeed, we found that Serca2a protein expression was reduced (by 30%) in RAP tissue, but the Serca2a/phospholamban (PLB) ratio was unchanged. PLB protein expression and its phosphorylation at Ser16 (PKA site) and Thr17 (CaMKII site) were also unchanged in RAP tissue (Supplemental Figure 8, A and B).

Sustained rapid atrial activation reduces RyR2 cluster size

Previous work has shown that even small increases in transverse RyR2 cluster distances can lead to complete failure of the centripetal Ca^{2+} wave in atrial myocytes (28). We therefore determined transverse RyR2 cluster distances in RAP cells. The mean and median (p50) transverse RyR2 cluster distances were unchanged in RAP compared with those in CTL cells (Figure 8, A and B). The heterogeneity index (HI) (p95-p5)/p50) and p95 of RyR2 cluster spacing were increased in RAP cells (Figure 8C). However, RyR2 protein expression levels were substantially reduced, and RyR2 phosphorylation at the primary PKA Ser2809 site was increased 7-fold (Figure 8D). Because of the magnitude of reduction of RyR2, we confirmed these results with different antibodies (Supplemental Figure 9). Furthermore, we performed additional semiquantitative RyR2 immunocytochemistry (Supplemental Figure 10), which further corroborated the reduction of RyR2 in RAP cells. Surprisingly, RyR2 phosphorylation at the predominant CaMKII site (Ser2814) was reduced (Figure 8D). The PKA-mediated phosphorylation of RyR2 at Ser2030 remained unchanged (Figure 8D). Thus, while RyR2 cluster distribution was largely unchanged in RAP, the significant reduction we observed in RyR2 protein expression suggests a substantially reduced RyR2 density per cluster.

Sustained rapid atrial activation does not increase CaMKII expression

Surprisingly, we found that cardiac CaMKII (CamKIIδ) and autophosphorylated CaMKII (Thr286) protein expression levels were not increased after RAP (Supplemental Figure 8D).

Sustained rapid atrial activation does not increase the Ca^{2+} spark rate

Ca^{2+} spark frequency and amplitude in the ss region were higher than in the central region of CTL atrial myocytes (Figure 9, A and

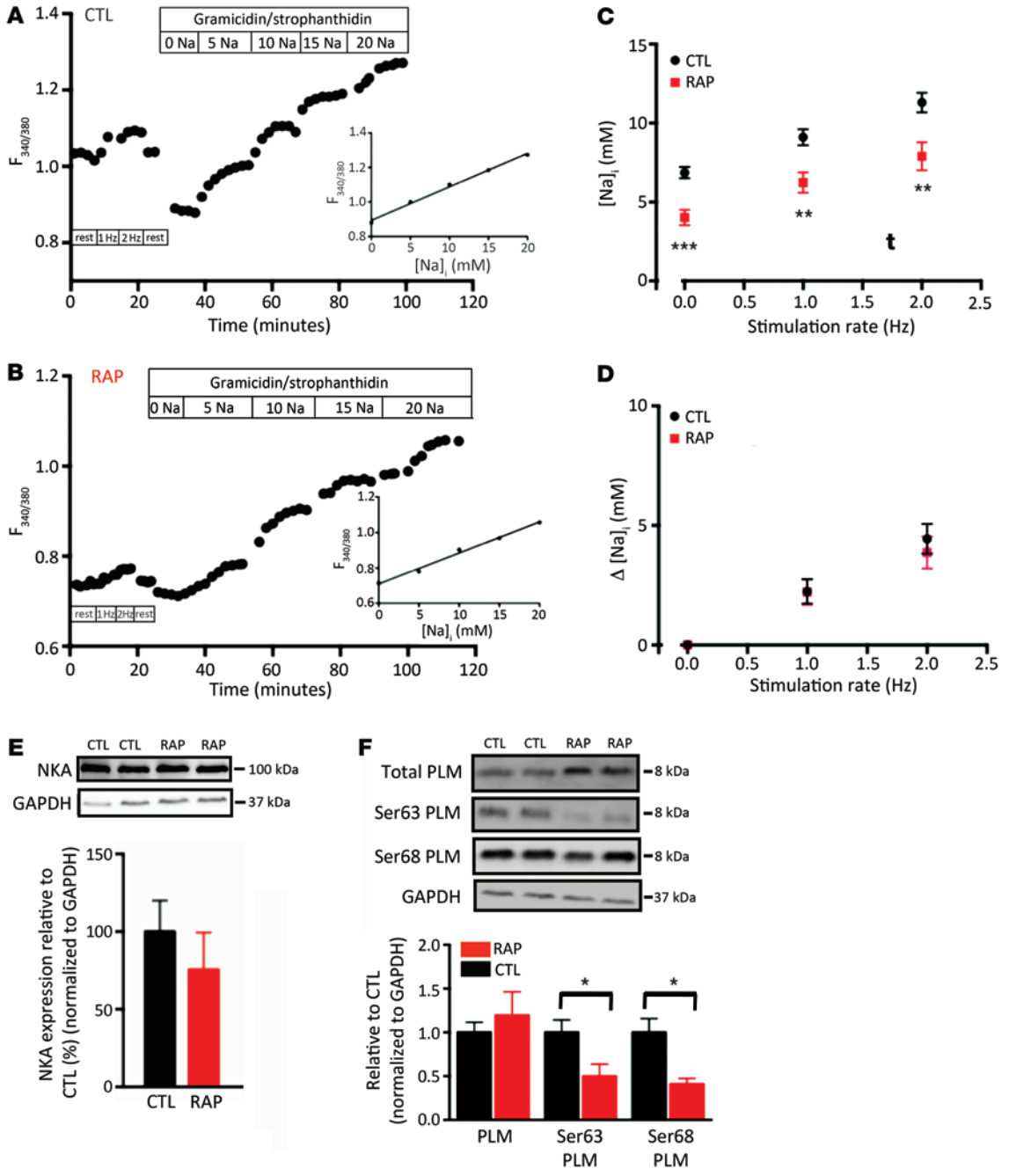

Figure 5. Altered Na⁺ homeostasis in RAP. (**A** and **B**) Representative ratiometric measurements of $[Na^+]_i$ in a CTL cell and an RAP cell with in situ calibration. (**C**) $[Na]_i$ at rest and during stimulation. $^{**}P < 0.01$; $^{***}P < 0.001$. (**D**) $\Delta[Na]_i$ in stimulated myocytes (CTL: 12 cells, 10 animals; RAP 9 cells, 7 animals). (**E**) Protein expression levels of NKA (NKA, CTL: $n = 15$; RAP: $n = 11$). (**F**) Protein expression levels of PLM and changes in PLM phosphorylation levels at Ser63 and Ser68 (CTL, PLM: $n = 15$, Ser63: $n = 14$, Ser68: $n = 15$; RAP, PLM: $n = 7$, Ser63: $n = 7$, Ser68: $n = 6$). $^{*}P < 0.05$.

B), similar to what has been observed in cat (21, 29) and rat atrial myocytes (30). Additionally, we found that Ca^{2+} spark mass and Ca^{2+} spark–mediated Ca^{2+} leak were also higher in the periphery compared with the central region (Figure 9, A and B). Surprisingly, these domain-specific Ca^{2+} spark characteristics did not change after RAP (Figure 9, A and B). Consistent with these findings, the inducibility and frequency of arrhythmogenic Ca^{2+} waves were also not altered in RAP cells (Figure 9, C and D). We found that β-adrenergic stimulation substantially increased Ca^{2+} wave frequencies in CTL and RAP cells (Figure 9D), and the increase was comparable in extent in both groups.

In order to investigate the seemingly paradoxical lack of increase in Ca^{2+} spark rates despite enhanced RyR2 phosphorylation, we performed computer simulations of intracellular Ca^{2+} signaling (Supplemental Figures 11 and 12 and ref. 31). Using a computational model of Ca^{2+} sparks and SR Ca^{2+} leak, we show that a reduction in RyR2 channel density that is consistent with the reduction of RyR2s in RAP (from 50 to 10 RyR2s per calcium

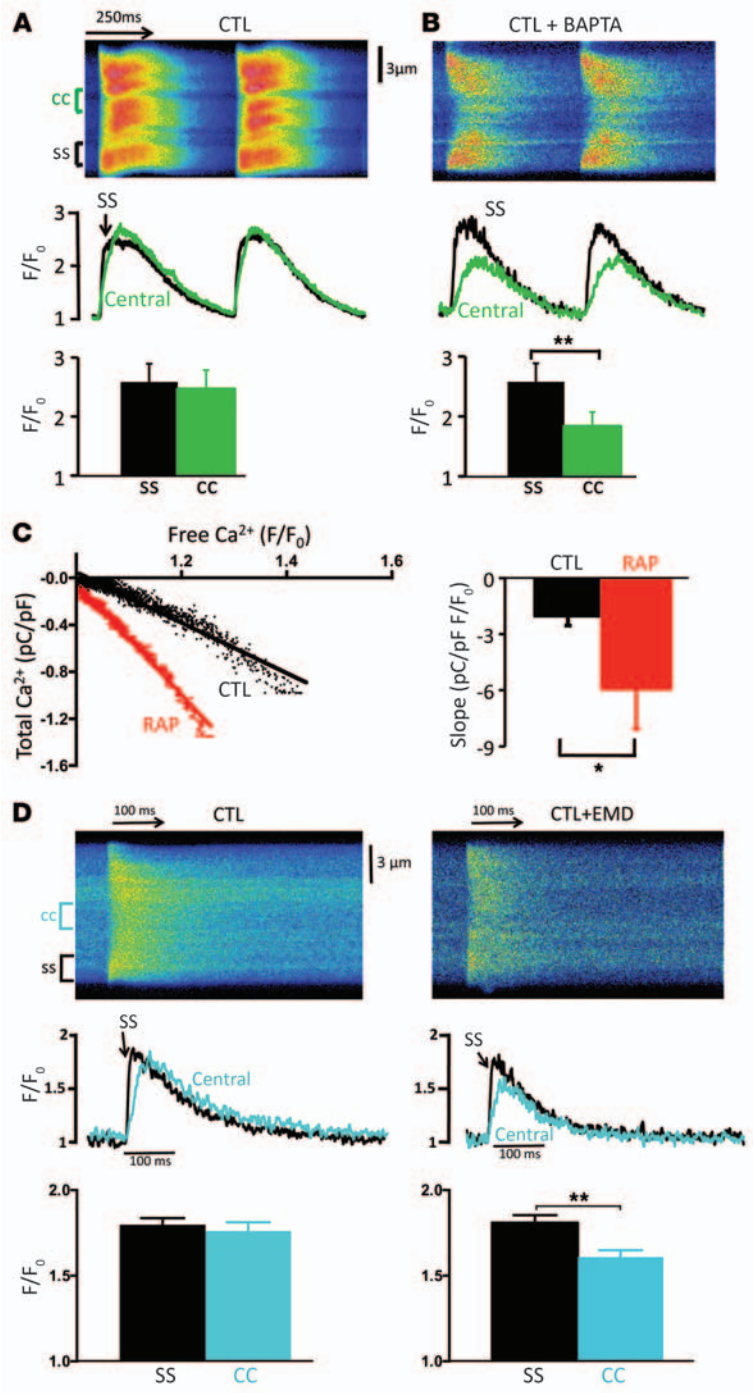

Figure 6. Intracellular Ca^{2+} buffering strength. Confocal linescans and derived local CaTs of a CTL cell (2 Hz) at baseline (**A**) and after application of 1 μmol of the Ca^{2+} chelator BAPTA-AM (n = 13 cells, 4 animals) (**B**). Similar ss and cc CaT amplitudes in CTL cells during steady-state stimulation (2 Hz) (**A**) and reduced cc CaT amplitude after treatment with 1 μmol/l BAPTA-AM (**B**). (**C**) Left panel: Example of intracellular Ca^{2+} buffering strength in an RAP cell and a CTL cell plotting the reverse $\int I_{NCX}$ (total Ca^{2+}) and the falling phase of the whole-cell CaT (epifluorescence, fluo-3; free Ca^{2+}) that were simultaneously recorded during fast application of caffeine (10 mmol/l). Right panel: Slopes of intracellular Ca^{2+} buffering strength in CTL versus RAP cells (CTL: n = 15 cells, 5 animals; RAP: n = 13 cells, 6 animals). (**D**) Confocal linescans of a CTL cell at baseline (left) and after addition of the Ca^{2+} sensitizer EMD (3 μmol/l) (n = 12 cells, 4 animals). *P < 0.05; **P < 0.01.

release unit [CRU]) results in an approximately 80% decrease in Ca^{2+} spark rates (Supplemental Figure 11C).

A doubling of the RyR2 channel open probability (P_O), resulting in a slight increase in RyR2 Ca^{2+} sensitivity, was estimated from constraining the model using the experimentally measured properties of Ca^{2+} spark rate and duration, SR Ca^{2+} load, and RyR2 cluster size from the present study (Supplemental Figure 11A). This estimated effect of increased RyR2 phosphorylation on Ca^{2+} sensitivity in RAP cells would balance out the changes induced by a reduced RyR2 cluster density to result in a Ca^{2+} spark rate (Supplemental Figure 11C) and SR Ca^{2+} load (Supplemental Figure 11B) similar to those in CTL cells (dotted blue line).

Ca^{2+} signaling silencing occurs in human AF

In field-stimulated (0.5 Hz) right atrial myocytes isolated from patients with persistent AF, the subcellular Ca^{2+} release pattern was similar to that in rabbit RAP cells. In human AF cells, we found that the cc CaT amplitude was significantly reduced compared with the ss CaT amplitude (Figure 10), while ss and cc CaT amplitudes were similar in CTL cells from patients with sinus rhythm (patient characteristics are shown in Supplemental Table 1).

Discussion

Sustained high atrial activation rate induces Ca^{2+} signaling silencing

In the present study, we have identified and characterized the Ca^{2+} signaling responses to a sustained high atrial activation rate in the absence of additional atrial or ventricular disease. Surprisingly, sustained rapid atrial activation does not produce arrhythmogenic intracellular Ca^{2+} signaling in healthy hearts, nor does it induce increases in CaMKII. Instead, a rapid rate alone produces Ca^{2+} signaling silencing. Ca^{2+} signaling silencing involves a constellation of changes at the cellular, molecular, and organizational levels, which act together to mitigate the actions of the high atrial rate with respect to Ca^{2+} instability. A key feature is the failure of centripetal intracellular Ca^{2+} wave propagation, which results in significantly reduced cc Ca^{2+} release and underlies the reduced whole-cell CaT. Other changes include an intricate remodeling of the RyR2 complex. We found that RyR2 protein expression was substantially decreased. RyR2 phosphorylation at the primary PKA site (Ser2809) was increased 7-fold, while phosphorylation at the primary CaMKII site (Ser2814) was reduced. We observed no changes in phosphorylation at the putative PKA site Ser2030. Importantly, low $[Na^+]_i$ was identified as a novel mechanism that contributes to the "unloading" of Ca^{2+} from RAP cells. Furthermore, we observed a 40% reduction in phosphorylated TnI (Ser23/24) and a 90% increase in calmodulin protein expression as well as a 180% increase in cytosolic fast Ca^{2+} buffering strength. Despite these vast changes in many Ca^{2+} cycling proteins, the rates of Ca^{2+} sparks and arrhythmogenic Ca^{2+} waves

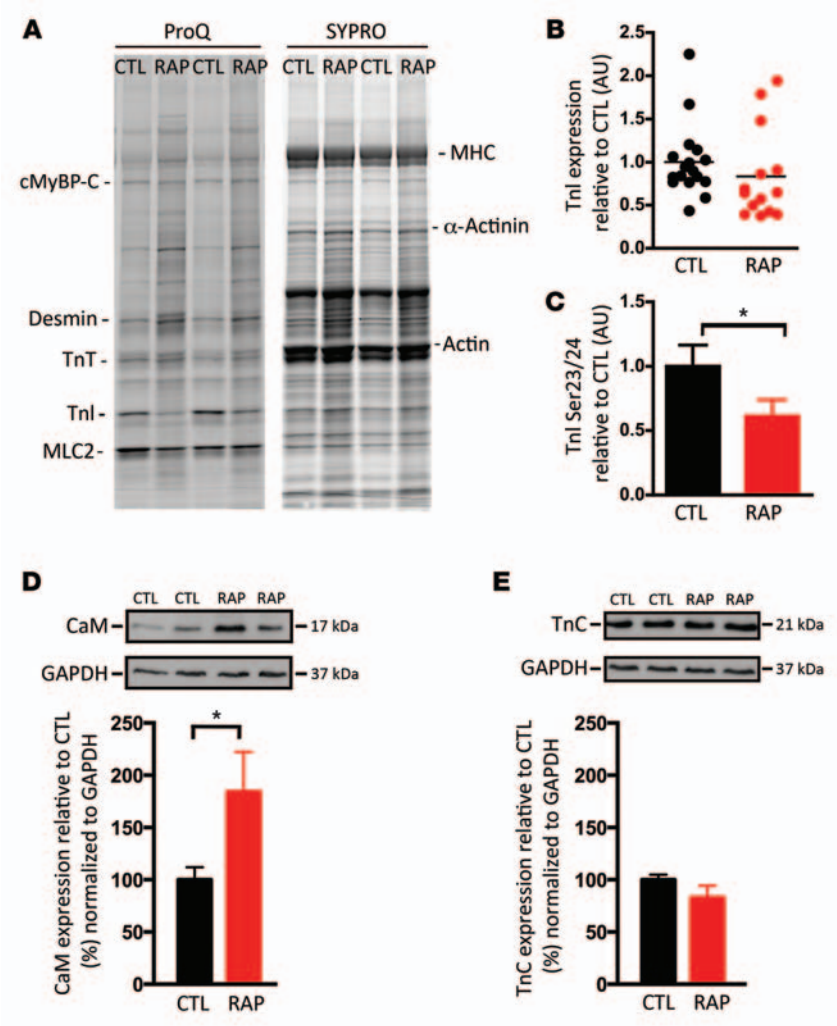

Figure 7. Fast [Ca^{2+}] buffering components. (**A**) Pro-Q Diamond staining (ProQ) to evaluate phosphorylation of myofilament proteins and SYPRO Ruby (SYPRO) to analyze total protein expression. cMyBP-C, cardiac myosin–binding protein C; TnT and TnI, cardiac TnT and TnI; MLC2, myosin light chain 2. (CTL: $n = 17$; RAP: $n = 14$.) (**B**) TnI protein expression. (**C**) Reduced TnI phosphorylation at Ser23/24 (CTL: $n = 17$; RAP; $n = 14$). (**D**) Increased calmodulin (CaM) and unchanged TnC protein expression levels (**E**) in RAP (relative to CTL and normalized to GADPH; CTL: $n = 15$; RAP: $n = 11$). *$P < 0.05$.

and the amount of Ca^{2+} spark–mediated Ca^{2+} leak from the SR were unchanged, thus we performed additional experiments to determine how this occurs. We deduced that during RAP, the number of RyR2s per SR RyR2 cluster must have decreased, since the number of SR RyR2 cluster sites and their transverse distance did not change, but single-cluster fluorescence was significantly reduced. The lower number of RyR2s per SR cluster was more active, as demonstrated by the high degree of phosphorylation of RyR2 at Ser2809. To evaluate the many changes and their effects on Ca^{2+} behavior, we performed a computational estimate of Ca^{2+} signaling in the atrial cells. The array of changes found after RAP accounts for the unchanged Ca^{2+} spark rate and is consistent with the low (unchanged) rate of Ca^{2+} waves and the reduced $[Ca^{2+}]_i$ transient in the center of the atrial cells that we observed. Furthermore, rapid atrial activation rates did not increase autophosphorylated CaMKII levels, which underlie the sustained increases in CaMKII activity, or CaMKII total protein expression.

We conclude that the unstable intracellular Ca^{2+} signaling that has been described in atrial myocytes from patients with persistent AF is not a consequence of the sustained high atrial activation rate per se. Specifically, the CaMKII-mediated Ca^{2+} signaling instability found in AF is not due to short periods of sustained high rates. Importantly, we show that a key feature of Ca^{2+} signaling silencing, the failure of intracellular Ca^{2+} wave propagation, is present in atrial myocytes isolated from patients with long-standing AF. It appears, therefore, that a stabilizing "silencing" remodeling of intracellular Ca^{2+} handling, which is described here for the first time to our knowledge, competes with arrhythmogenic Ca^{2+} instability in AF. Despite this important conclusion, our findings raise a number of questions that focus on the roles of the TT system, $[Na_i]$, fast Ca^{2+} buffers, the hyperphosphorylation paradox, and alterations in $I_{Ca,L}$ and NCX.

Ca^{2+} signaling silencing is not due to TT depletion. Compared with ventricular myocytes, atrial myocytes have few TTs (32). In the present study, we found that rabbit and human left atrial myocytes have a similar, nominal TT content. In CTL rabbit and human atrial myocytes, this results in nonuniform intracellular Ca^{2+} signaling, as described previously in atrial cells (3, 21). In the present study, mouse left atrial myocytes had a substantial TT density comparable to the values described for larger mammals (e.g., sheep, dog) (12, 13). Recent work in human right atrial tissue has shown the presence of TTs, albeit less abundant than in other large mammals (cow, horse, sheep) (33). A denser TT system leads to more DHPR-RyR2 pairs at the junctional SR (jSR), thus facilitating (near-) simultaneous CaT activation throughout the cell (34). In the present study, ss and cc CaT amplitudes were the same in CTL cells. After RAP, cc CaT amplitudes were significantly reduced, but ss CaT amplitudes were unchanged. Although RAP cells were wider than CTL cells, the failure of intracellular Ca^{2+} wave propagation was not correlated with cell width (Supplemental Figure 4). Reduced central CaTs have been previously described in atrial myocytes in an ovine heart failure model (34) (which predisposes to AF) and a canine RAP model (13). Atrial myocytes in these models showed significant TT depletion, thus reducing DHPR-RyR2 pairs. In an ovine model of AF, TT depletion also significantly reduced the number of DHPR-RyR2 pairs, which resulted in reduced EC coupling in these cells (12). Thus, in species with functionally important atrial TTs (sheep, dog), TT depletion is an important mechanism of altered Ca^{2+} signaling in various models of atrial remodeling. In the present study, however, in atrial myocytes without TTs, reduced central CaTs occurred independently of changes in TT abundance. In our study, isolated human left atrial myocytes did not have functionally relevant TTs in either the CTL or AF myocytes. Therefore, taken together with previous studies, our results indicate that further work needs to be performed to

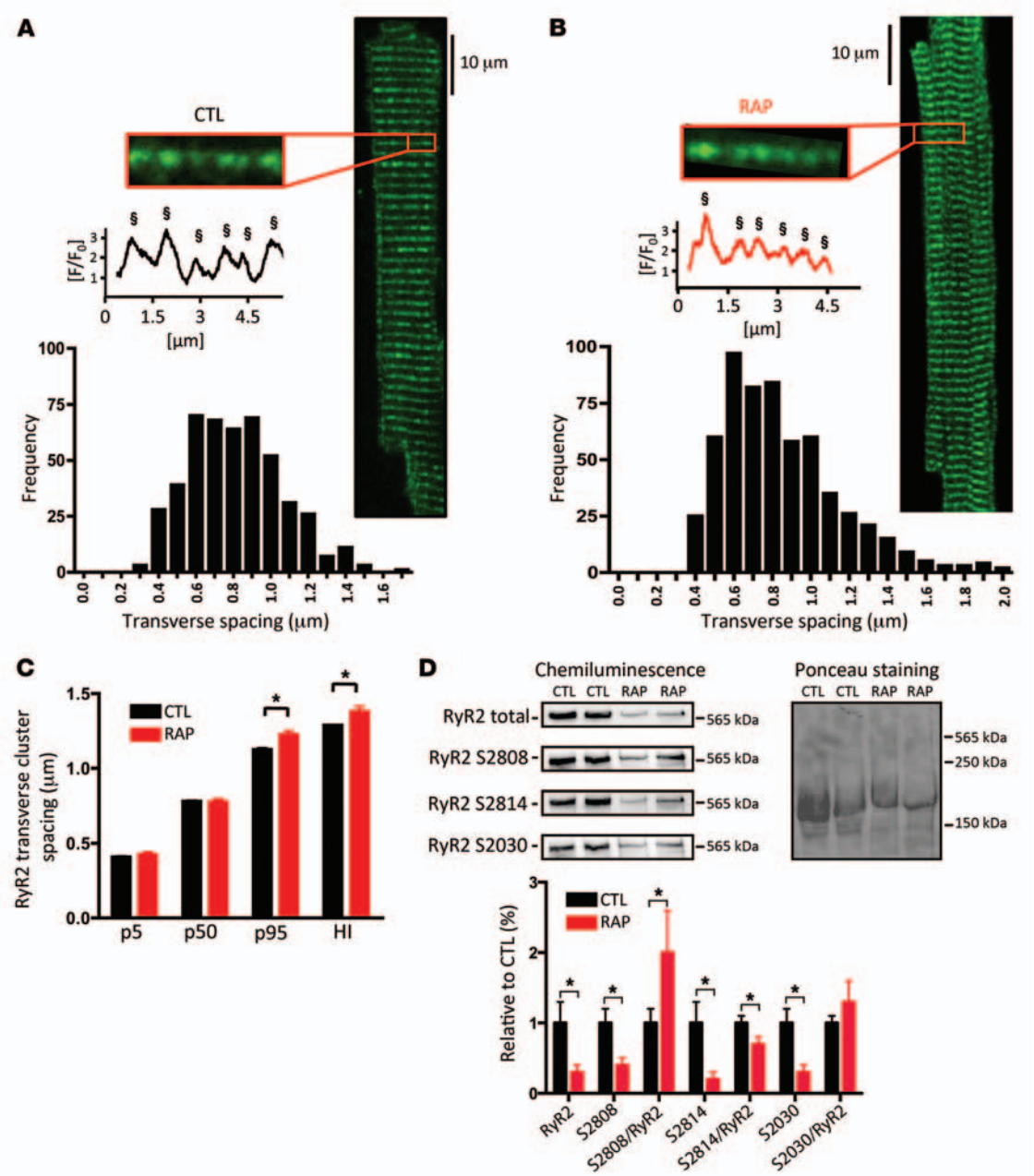

Figure 8. RyR2 in atrial myocytes. (**A**) Confocal immunofluorescence image of RyR2 clusters in a CTL cell. (**B**) As in **A**, but with an RAP cell. Both panels show transverse spacing of RyR2 clusters. Enlarged panels show the region of interest (ROI) that was used to obtain the transverse RyR2 cluster distance. Below are the intensity profiles along each ROI. §, denotes the peaks of intensity, and their distance is measured as the spacing between the RyR2 clusters. Representative histograms of transverse RyR2 cluster spacing from 1 animal (10 cells). (**C**) Percentiles and heterogeneity index (p95-p5/p50) for CTL and RAP cells (CTL: 408 ROI, n = 51 cells, n = 8; RAP: 420 ROIs, n = 60 cells, n = 8). (**D**) Western blot analyses showing changes in total RyR2 protein expression and phosphorylation in RAP cells (CTL: n = 18; RAP: n = 15). n = number of animals. *P < 0.05.

understand whether TT depletion alters Ca^{2+} signaling in human AF. Additionally, the substantial density of TTs in left atrial mouse cells suggests that TT density is highly species dependent.

Sustained RAP increases intracellular Ca^{2+} buffering strength. The regenerative centripetal intracellular Ca^{2+} wave in atrial myocytes relies on the activation of central RyR2 clusters by Ca^{2+} diffusion from more peripheral sites (21). Increasing the cell's fast buffering strength, which contributes to the dynamic regulation of $[Ca]_i$ (35, 36), has been shown to lead to a failure of the centripetal regenerative Ca^{2+} wave (37). In the present study, treatment of CTL cells with the fast Ca^{2+}-chelating agent BAPTA reproduced these findings. Thus, we found that increasing the fast Ca^{2+} buffering strength in CTL cells leads to a failure of the centripetal Ca^{2+} wave similar to that seen in RAP cells. The fast Ca^{2+} buffering strength was significantly increased in atrial myocytes after RAP.

We found that TnI phosphorylation (Ser23/24) in RAP was significantly reduced. This increased myofilament Ca^{2+} sensitivity (and thus TnC Ca^{2+} binding)(25) and therefore augmented the fast Ca^{2+} buffering strength. Myofilament Ca^{2+} binding can constitute up to 50% of the cardiac myocyte's fast Ca^{2+} buffering strength

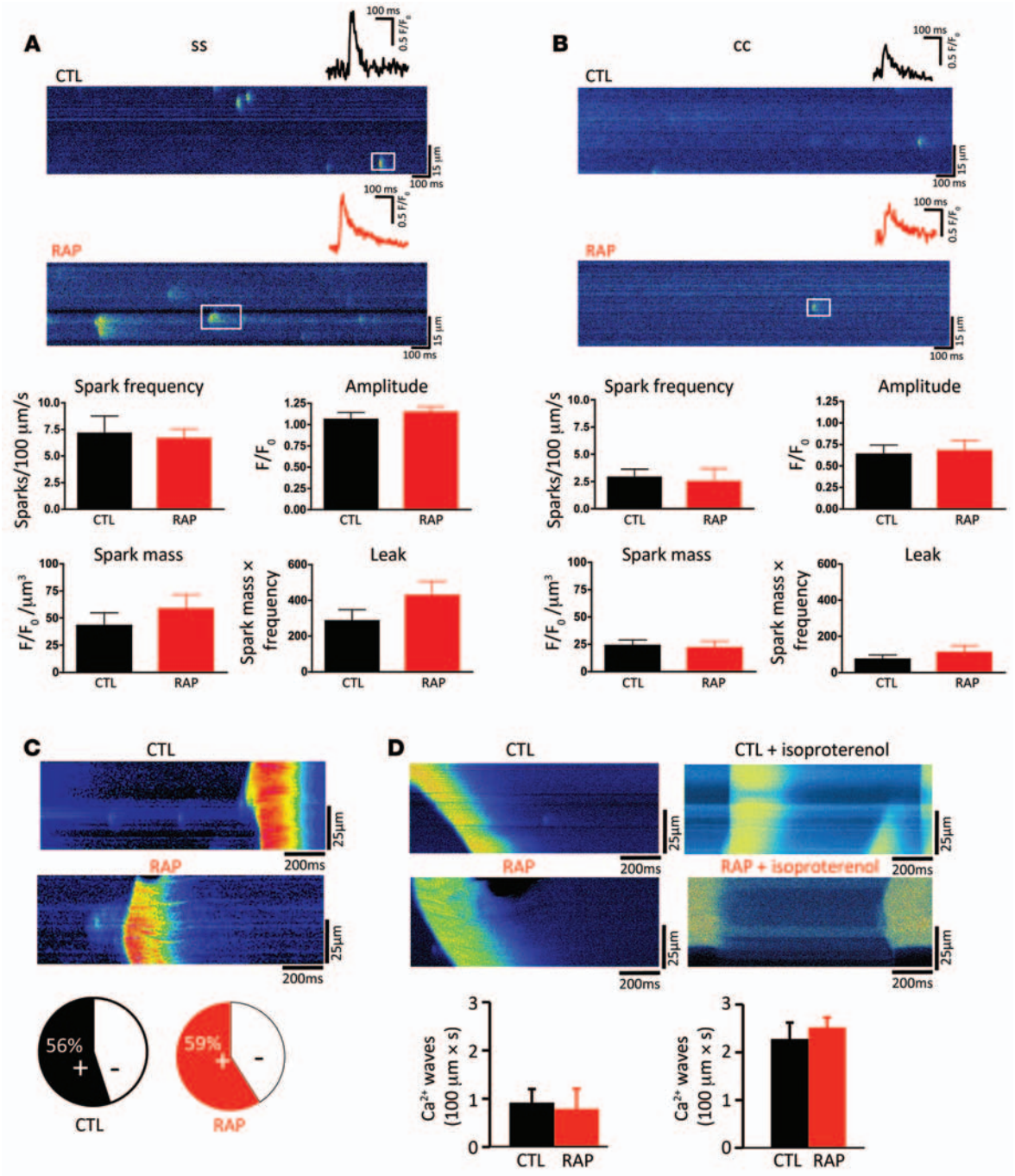

Figure 9. Ca^{2+} sparks and Ca^{2+} waves. (**A**) Ca^{2+} spark frequency, amplitude, mass, and Ca^{2+} spark–mediated Ca^{2+} leak in a CTL cell in ss (CTL: *n* = 250, 21 cells, 5 animals; RAP: *n* = 210, 19 cells, 5 animals) and cc (CTL: *n* = 80, 21 cells, 5 animals; RAP: *n* = 90, 19 cells, 5 animals) domains. (**B**) As in **A** for RAP cells. ss (*n* = 210, 19 cells, 5 animals) and cc (*n* = 90, 19 cells, 5 animals) regions. (**C**) Ca^{2+} wave inducibility (CTL: *n* = 33 cells, 6 animals; RAP: *n* = 34 cells, 6 animals). (**D**) Ca^{2+} wave frequency at baseline and after stimulation with 1 µmol/l isoproterenol in the same cell (CTL: *n* = 25 cells, 5 animals; RAP: *n* = 22 cells, 5 animals).

(35). Indeed, treatment of CTL cells with the Ca^{2+} sensitizer EMD, which increases fast Ca^{2+} buffering (27), showed a significant reduction of the central CaT amplitude without changes in the ss CaT amplitude. These results show that in atrial myocytes without relevant TTs, increased myofilament sensitivity results in significantly reduced Ca^{2+} release in the center of the cell. Increases in Ca^{2+} sensitivity have been reported for skinned fibers from an RAP model in dogs (13) and from AF patients (38), suggesting increased fast Ca^{2+} buffering in these cells. Furthermore, a modeling study in atrial myocytes without TTs found that increases in TnC (and thus myofilament Ca^{2+} sensitivity) induced a profound decrease in Ca^{2+} signals in the center of the myocyte (23). This suggests an important role for myofilament-mediated Ca^{2+} binding in centripetally propagating Ca^{2+} wave regulation in atrial myocytes. Here, we identify fast Ca^{2+} buffering strength as an important, novel modulator of atrial intracellular Ca^{2+} signaling, one that serves as an adaptive

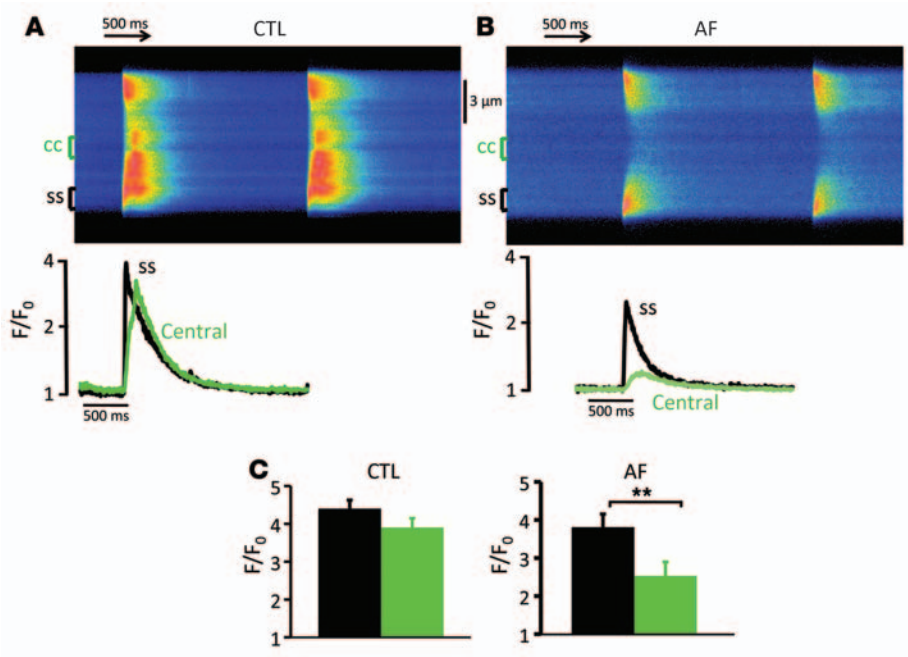

Figure 10. Ca^{2+} signaling silencing in human AF. (**A**) Representative transverse confocal linescan and derived local CaTs from a CTL cell (patient in sinus rhythm) during steady-state field stimulation (0.5 Hz) showing similar amplitudes of ss and cc CaTs. (**B**) As in **A** for an AF cell showing the significantly blunted cc CaT. (**C**) Reduced cc but preserved ss CaT amplitude in human AF cells (CTL: n = 39 cells, 9 patients; AF: n = 23 cells, 10 patients). $^{**}P < 0.01$.

compensatory mechanism after sustained increases in activation rates and a crucial component of Ca^{2+} signaling silencing.

Rapid atrial activation results in a RyR2 "hyperphosphorylation paradox." The distinct mechanisms underlying Ca^{2+}-induced Ca^{2+} release in the ss and central domains of atrial myocytes also affect domain-specific Ca^{2+} sparks. Previous work in cat atrial myocytes (37) and data from the present study show that Ca^{2+} spark frequency is significantly higher in the ss domain compared with the center of atrial myocytes (29). Surprisingly, sustained high atrial activation rates during RAP did not alter domain-specific Ca^{2+} spark frequencies, although atrial RyR2 phosphorylation levels were significantly increased. Studies in atrial myocytes from patients with AF have shown increased global Ca^{2+} spark (7, 39) and wave frequencies (39). Increased RyR2 phosphorylation is a characteristic finding in human AF (5, 6, 40) and AF models (41). Bilayer studies of atrial RyR2 isolated from patients with AF showed increases in P_O due to increased phosphorylation at Ser2809 (6), a primary PKA (6) phosphorylation site. Phosphorylation-mediated RyR2 sensitization has been implicated in underlying increased Ca^{2+} spark frequency and diastolic Ca^{2+} leak in AF. Indeed, treatment with a CaMKII inhibitor normalized increased Ca^{2+} spark frequency and diastolic Ca^{2+} leak in human atrial myocytes from AF patients, with increased RyR2 phosphorylation at a CaMKII site (Ser2814) (7), and reduced the number of delayed after depolarizations (DADs) recorded in atrial myocytes from patients with AF (5). Interestingly, in the present study, RyR2 phosphorylation at this primary CaMKII site (Ser2814) was reduced. While increases in RyR2 phosphorylation at a primary PKA site (Ser2809) exceeded those found in human AF (6), we detected no increases in Ca^{2+} spark and Ca^{2+} wave frequencies or Ca^{2+} spark–mediated Ca^{2+} leak.

Computer simulations using an existing physiological model of Ca^{2+} sparks and SR Ca^{2+} leak (31) showed a significant (~80%) reduction in Ca^{2+} spark frequency for the degree of RyR2 channel reduction found after RAP. To keep Ca^{2+} spark rates and SR Ca^{2+} content normal in RAP despite a reduced RyR2 cluster size, RyR2 Ca^{2+} sensitivity has to increase. Computational estimates show that this increase in RyR2 Ca^{2+} sensitivity due to the putative effects of increased RyR2 phosphorylation at the PKA site Ser2804 would be achieved by a 2-fold increase in RyR2 P_O. Our study provides strong evidence that increased RyR2 phosphorylation alone does not equate with an increase in Ca^{2+} spark frequency and that the RyR2 channel density per cluster is an equally important determinant of Ca^{2+} spark frequency. RyR2 protein expression was reduced in human AF (7) and in an ovine AF model (12), but to a lesser degree (~ 45% and 20%, respectively), while a recent study found no change in RyR2 protein expression in human AF (5). Computer simulations from the present study indicated that moderate RyR2 reduction, as reported for persistent AF, together with increased phosphorylation, would result in increased Ca^{2+} spark rates (as has been experimentally shown for AF). Thus, the substantial RyR2 channel reduction per cluster induced by sustained rapid atrial activation is an important part of the Ca^{2+} signaling silencing response. It counteracts the effects of increased RyR2 phosphorylation and prevents an increase in Ca^{2+} spark rates above those of CTLs. β-adrenergic stimulation led to similar increases in arrhythmogenic Ca^{2+} waves in CTL and RAP cells, providing further evidence for an unchanged Ca^{2+} release threshold in RAP.

Surprisingly, we found that protein expression levels for CaMKII and autophosphorylated CaMKII (CaMKIIpTh286) were not increased by RAP. Increased CaMKII expression has been documented in atria of AF patients (7, 8) and has been found to contribute to unstable Ca^{2+} signaling during AF (5, 7). In a previous RAP study in dogs, CaMKIIδ and CaMKIIpTh286 protein expression were increased in the right atrium (13), however, RyR2 phosphorylation at the primary CaMKII site Ser2814 was unchanged. Thus, a rapid rate alone does not appear to produce the increase in RyR2 phosphorylation at the CaMKII site Ser2814 that appears to be important for the unstable intracellular Ca^{2+} signaling seen in AF.

Steady-state phosphorylation is determined by the balance between protein kinases and phosphatases, which are fine-tuned within the RyR2 macromolecular complex by regulatory proteins (42). This allows specific targeting of phosphorylation sites located in close proximity. Future studies are necessary to unravel the exact mechanisms of the complex regulatory machinery within the RyR2 complex.

$I_{Ca,L}$ reduction in RAP

Studies in human and cat atrial myocytes have shown that only ss CaTs are under the tight control of $I_{Ca,L}$ (37, 43). CaTs in the central region, due to their activation by the centripetally propagating Ca^{2+} wave, are relatively independent of $I_{Ca,L}$ (37). $I_{Ca,L}$ reduction, which is a hallmark of AF-induced remodeling (14, 15), was therefore thought to lead to a reduction in ss CaTs and thus to contribute to Ca^{2+} signaling silencing. Indeed, we show that pharmacological reduction of $I_{Ca,L}$ in CTL cells reduces ss CaTs. However, cc CaTs had amplitudes similar to those of ss CaTs, showing that the centripetal intracellular Ca^{2+} wave was not interrupted. Interestingly, in RAP myocytes, ss CaTs were not reduced despite a significant reduction in $I_{Ca,L}$. A similar preservation of ss CaTs was found in an ovine AF (12) and a canine RAP model (13), albeit with lesser reductions in $I_{Ca,L}$. Ca^{2+} sensitization due to RyR2 hyperphosphorylation could contribute to facilitated SR Ca^{2+} release in the ss domain (44). In line with this hypothesis, our simulations indicated an increased Ca^{2+} sensitivity of RyR2 after RAP. Ca^{2+} spark frequency, however, and Ca^{2+} spark–mediated Ca^{2+} leak were unaltered. While RyR2 protein expression was significantly reduced after RAP, the cluster distribution remained unchanged. Thus, the number of RyR2 channels per cluster and, therefore, the signal mass upon cluster activation are likely reduced in RAP, but might be different between ss and central domains. Future studies addressing cluster-specific ultrastructure are needed to elucidate this question.

Sustained rapid rate lowers $[Na^+]_i$

$[Na^+]_i$ is a potent regulator of intracellular Ca^{2+} signaling, and altered $[Na^+]_i$ is an important mechanism of Ca^{2+} dysregulation in heart disease. For example, high $[Na^+]_i$ has long been recognized as an important part of Ca^{2+} dysregulation in heart failure (45). The present study is the first to our knowledge to determine $[Na^+]_i$ in viable atrial cells. We have uncovered low $[Na^+]_i$ as an important novel mechanism contributing to "Ca^{2+} unloading" during rapid activation rates, mainly by activation of NCX-mediated Ca^{2+} extrusion (see below) during reduced I_{Ca} entry. Calculations of Ca^{2+} and Na^+ fluxes over 1 activation cycle show that the substantial reduction in Ca^{2+} entry (reduced $I_{Ca,L}$ and shortened AP) leads to a significant reduction in Na^+ entry through the NCX. During 1-Hz stimulation, 4 times as much Na^+ enters the cell through the NCX than through Na^+ channels (18). The reduced phosphorylation levels of the NKA regulatory protein PLM are possibly a compensatory effect of reduced Na^+ entry through the NCX. Thus, Ca^{2+} signaling silencing entails "Na^+ signaling silencing" by substantially reduced Na^+ entry and a compensatory reduction in NKA activity. Previous work by Akar et al. also described reduced subcellular and whole-cell Na^+ using electron probe microanalysis in snap-frozen left atrial tissue from dogs that underwent 48 hours of RAP (2).

Low $[Na^+]_i$ is an important part of Ca^{2+} signaling silencing and may represent a general response of cardiac myocytes to rapid stimulation rates during tachycardia.

Changes in NCX function

While NCX protein expression is the same in CTL and RAP atrial myocytes, the sensitivity of I_{NCX} to $[Ca^{2+}]_i$ is much greater in RAP cells. One important underlying mechanism is the low $[Na^+]_i$ in RAP cells. Small changes in $[Na^+]_i$ already substantially alter NCX activity (45). In intact RAP cells, the reduced $[Na^+]_i$ increases NCX-mediated Ca^{2+} extrusion compared with CTLs by activation of forward-mode NCX, which is reflected in a faster decay of the caffeine-induced CaT. Whether the increase in NCX activity that was measured in patched cells, where $[Na^+]_i$ is held constant, is also caused by low $[Na^+]_i$ depends on the $[Na^+]_i$ that is sensed in the dyadic cleft. Previous work has shown that local $[Ca^{2+}]_i$ in the dyadic cleft is generated by the activation of different ion currents ($I_{Ca,L}$, I_{Na}) and pumps (NCX, Na^+/K^+ pump) (46). It follows that the localized cleft $[Ca^{2+}]_i$ also results in localized $[Na^+]_i$. In addition, diffusion of Na^+ in cardiac myocytes was found to be slow, which contributes to a localized $[Na^+]_i$ in the dyadic cleft (47). Whether other "activators" or "sensitizers" of NCX further contribute to the increase in NCX activity in RAP cells will need to be tested in additional experiments.

The functional implications of enhanced NCX function at any given $[Ca^{2+}]_i$ are important. Since there is the same amount of NCX protein in RAP cells, this property of NCX would lead to a lower $[Ca^{2+}]_i$ in these cells if all other determinants of NCX activity were equal. They are, however, not equal. The time course of the $[Ca^{2+}]_i$ transient in the ss domain near NCX is more rapid. Thus, although the NCX exchanges Na^+ against Ca^{2+} more rapidly, they are exposed to high $[Ca^{2+}]_i$ for a shorter period of time. The similar amount of Ca^{2+} in the SR suggests that when averaged over time, the entry and extrusion of Ca^{2+} into and out of the cell are equal. Overall, these features are consistent with the other elements of Ca^{2+} signaling silencing. The increased sensitivity of NCX to $[Ca^{2+}]_i$ actually appears to be an adaptive (and beneficial) mechanism when RAP cells are driven at a high rate. With a high rate, the Ca^{2+} entry will be greater due to the repetitive activation of $I_{Ca,L}$, even when the $I_{Ca,L}$ amplitude is smaller. With greater Ca^{2+} entry, NCX in the RAP cells is better able to balance that high influx with a relatively higher efflux of Ca^{2+} than would be the case if NCX $[Ca^{2+}]_i$ sensitivity were the same as it is in CTL cells.

Clinical relevance and Ca^{2+} silencing in AF

The present study shows for the first time to our knowledge that sustained rapid rates that occur in a prodrome to AF as episodes of paroxysmal AF actually counteract the development of arrhythmogenic Ca^{2+} instability. This implies that the net changes in Ca^{2+} signaling seen in a specific patient are a consequence of both Ca^{2+} signaling silencing and Ca^{2+} signaling instability. It appears that, in some patients, the effects of Ca^{2+} signaling silencing prevail, as shown in our data from human AF. Failure of the centripetal intracellular Ca^{2+} wave, which is a key feature of Ca^{2+} signaling silencing and is caused by a complex remodeling of intracellular Ca^{2+} signaling, is observed in field-stimulated intact atrial cells from patients with persistent AF. Similarly, some authors also reported reduced, rather than enhanced, spontaneous ectopic activity in isolated

atrial trabeculae from patients with persistent AF compared with patients with sinus rhythm (48, 49). Consistent with the concept of Ca^{2+} signaling silencing, lone rapid atrial pacing or experimental AF as such has never been shown to produce an enhanced rate of atrial ectopic activity, nor has spontaneous recurrence of AF been documented, even after prolonged periods of AF (10). A heart failure model in dogs, on the other hand, produced unstable atrial Ca^{2+} signaling, resulting in increased DADs in atrial myocytes (11).

Summary

We identify and characterize Ca^{2+} signaling silencing as a novel adaptive response to a sustained high atrial activation rate in the absence of additional atrial disease. Ca^{2+} signaling silencing is characterized by an intricate array of cellular and molecular changes and organizational remodeling that attenuate the effects of a sustained high atrial rate with respect to Ca^{2+} signaling instability. We further provide evidence that key features of Ca^{2+} signaling silencing are present in long-standing human AF.

Our results show that in patients with AF, net changes in Ca^{2+} signaling are likely a balance between Ca^{2+} signaling instability and Ca^{2+} signaling silencing. In some AF patients, in whom spontaneous ectopic activity in isolated trabeculae was reduced, the effects of Ca^{2+} signaling silencing appear to prevail (48, 49).

Methods

Rapid atrial pacing model and isolation of atrial myocytes. New Zealand White rabbits were rapidly stimulated for 5 days in the right atrium via implanted pacemaker leads connected to an external pacemaker. Sham-operated animals served as CTLs. A detailed description of the animal model and atrial cell isolation can be found in the Supplemental Methods.

Intracellular Ca^{2+} measurements. For ratiometric fluorescence measurements using whole-cell epifluorescence, cells were loaded with 2 to 10 μmol/l of the Ca^{2+} indicator fura-2-acetoxymethyl ester (Fura-2-AM; Invitrogen) for 20 minutes at room temperature. Cells were mounted on an inverted microscope (Nikon TE2000-S) and stimulated via external field stimulation (2 Hz, 37°C) (MyoPacer; IonOptix). Fura-2 was alternately excited at 340 and 380 nm every 2 ms using an argon lamp (Cairn), and emitted fluorescence (510 ± 40 nm) was collected via a ×40/1.3 numerical aperture (NA) objective. The raw 340 nm, 380 nm, and 340:380 ratio signals were sampled at 1 kHz (CED 1401 A/D converter) and displayed, stored, and analyzed using IonWizard software (IonOptix). The 340:380 fluorescence ratio was taken as an index of intracellular $[Ca^{2+}]$.

For confocal microscopy, cells were seeded on laminin-coated glass coverslips and loaded for 20 minutes with 10 μmol/l of the Ca^{2+} indicator fluo-4-acetoxymethyl ester (Fluo-4-AM; Invitrogen). After allowing 20 minutes for de-esterification, cells were mounted on an inverted microscope (Nikon TE2000-U). The Ca^{2+} indicator was excited with the 488 nm line of an argon ion laser attached to the microscope via a confocal laser scanning unit (Nikon C1). Emitted fluo-4 fluorescence was measured at wavelengths of greater than 515 nm. Linescan images (1.5–3 ms $line^{-1}$, pixel size 0.1 μm) were recorded from a central focal plane. The scanned line was oriented in the transverse direction, i.e., perpendicularly to the longitudinal axis of the cell. For evaluation of local subcellular Ca^{2+} release, the ss domain was defined as 2 μm beneath the outer cell membrane in the transverse linescan direction. For the determination of arrhythmogenic Ca^{2+} waves, longitudinal linescans were performed.

A more detailed description of all experimental protocols (including additional whole-cell epifluorescence measurements using fluo-3) and analyses can be found in the Supplemental Methods.

Statistics. Results are reported as means ± SEM for the indicated number of cells, animals, or Ca^{2+} sparks unless otherwise indicated. Statistical analyses were performed using a 2-tailed Student *t* test for unpaired values or repeated-measures 2-way ANOVA as appropriate. Values of $P < 0.05$ were considered statistically significant.

Study approval. Animal handling was performed according to the European directive on laboratory animals (86/609/EEC). The study protocol was approved by the ethics committee for animal research at Maastricht University (DEC). The investigation conformed with NIH guidelines (*Guide for the Care and Use of Laboratory Animals*. NIH publication no. 85-23. Revised 1996). All patients provided written informed consent prior to surgery. The study protocols were approved by the IRB of the University of Maryland and the medical ethics committee of Maastricht University (MEC 2010-2004).

Acknowledgments

We thank Joseph Kao for discussion and help with the estimation of intracellular BAPTA concentrations. This study was supported by a Scientist Development Grant from the American Heart Association (14SDG20110054, to M. Greiser); the Dutch Heart Foundation (2005B112, U. Schotten); the Dutch Research Organization (NWO) (VIDI-grant 016.086.379, to U. Schotten); the Leducq Foundation (European-North American Atrial Fibrillation Research Alliance [ENAFRA]) (to U. Schotten, D. Dobrev, U. Ravens, M.A. Allessie, and W.J. Lederer); the European Union (European Network for Translational Research in Atrial Fibrillation [EUTRAF]) (261057, to U. Schotten, D. Dobrev, and U. Ravens); the National Heart, Lung, and Blood Institute (NHLBI) (R01 HL106059, R01 HL105239-01, and P01 HL67849, to W.J. Lederer); and the German Centre for Cardiovascular Research (DZHK) (to D. Dobrev). In addition, the research leading to these results has received funding from the European Community's Seventh Framework Programme FP7/2007–2013 under grant agreement HEALTH-F2-2009-241526, EUTrigTreat (to W.J. Lederer).

Address correspondence to: Maura Greiser or Ulrich Schotten, Department of Physiology, Maastricht University, P.O. Box 616, 6200MD Maastricht, The Netherlands. Phone: 31.43.3881320; E-mail: mgreiser@umaryland.edu (M. Greiser), schotten@maastrichtuniversity.nl (U. Schotten).

1. Elvan A, et al. Dominant frequency of atrial fibrillation correlates poorly with atrial fibrillation cycle length. *Circ Arrhythm Electrophysiol*. 2009;2(6):634–644.
2. Akar JG, et al. Intracellular chloride accumulation subcellular elemental distribution during atrial fibrillation. *Circulation*. 2003;107(13):1810–1815.
3. Greiser M, Schotten U. Dynamic remodeling of intracellular Ca(2+) signaling during atrial fibrillation. *J Mol Cell Cardiol*. 2013;58:134–142.
4. Greiser M, Lederer WJ, Schotten U. Alterations of atrial Ca(2+) handling as cause consequence of atrial fibrillation. *Cardiovasc Res*. 2011;89(4):722–733.
5. Voigt N, et al. Enhanced sarcoplasmic reticulum Ca^{2+} leak increased Na^{+}-Ca^{2+} exchanger function

underlie delayed afterdepolarizations in patients with chronic atrial fibrillation. *Circulation*. 2012;125(17):2059–2070.
6. Vest JA, et al. Defective cardiac ryanodine receptor regulation during atrial fibrillation. *Circulation*. 2005;111(16):2025–2032.
7. Neef S, et al. CaMKII-dependent diastolic SR Ca^{2+} leak elevated diastolic Ca^{2+} levels in right atrial myocardium of patients with atrial fibrillation. *Circ Res*. 2010;106(6):1134–1144.
8. Tessier S, et al. Regulation of the transient outward K(+) current by Ca(2+)/calmodulin-dependent protein kinases II in human atrial myocytes. *Circ Res*. 1999;85(9):810–819.
9. De Koninck P, Schulman H. Sensitivity of CaM kinase II to the frequency of Ca^{2+} oscillations. *Science*. 1998;279(5348):227–230.
10. Schotten U, Verheule S, Kirchhof P, Goette A. Pathophysiological mechanisms of atrial fibrillation: a translational appraisal. *Physiol Rev*. 2011;91(1):265–325.
11. Yeh YH, et al. Calcium-handling abnormalities underlying atrial arrhythmogenesis and contractile dysfunction in dogs with congestive heart failure. *Circ Arrhythm Electrophysiol*. 2008;1(2):93–102.
12. Lenaerts I, et al. Ultrastructural and functional remodeling of the coupling between Ca^{2+} influx sarcoplasmic reticulum Ca^{2+} release in right atrial myocytes from experimental persistent atrial fibrillation. *Circ Res*. 2009;105(9):876–885.
13. Wakili R, et al. Multiple potential molecular contributors to atrial hypocontractility caused by atrial tachycardia remodeling in dogs. *Circ Arrhythm Electrophysiol*. 2010;3(5):530–541.
14. Van Wagoner DR, Pond AL, Lamorgese M, Rossie SS, McCarthy PM, Nerbonne JM. Atrial L-type Ca^{2+} currents human atrial fibrillation. *Circ Res*. 1999;85(5):428–436.
15. Christ T, et al. L-type Ca^{2+} current downregulation in chronic human atrial fibrillation is associated with increased activity of protein phosphatases. *Circulation*. 2004;110(17):2651–2657.
16. Sipido KR, Wier WG. Flux of Ca^{2+} across the sarcoplasmic reticulum of guinea-pig cardiac cells during excitation-contraction coupling. *J Physiol*. 1991;435:605–630.
17. Trafford AW, Díaz ME, Eisner DA. Coordinated control of cell Ca(2+) loading triggered release from the sarcoplasmic reticulum underlies the rapid inotropic response to increased L-type Ca(2+) current. *Circ Res*. 2001;88(2):195–201.
18. Despa S, Islam MA, Pogwizd SM, Bers DM. Intracellular [Na+] and Na+ pump rate in rat and rabbit ventricular myocytes. *J Physiol*. 2002; 539(pt 1):133–143.
19. Despa S, et al. Phospholemman-phosphorylation mediates the β-adrenergic effects on Na/K pump function in cardiac myocytes. *Circ Res*. 2005;97(3):252–259.
20. Han F, Bossuyt J, Despa S, Tucker AL, Bers DM. Phospholemman phosphorylation mediates the protein kinase C-dependent effects on Na^+/K^+ pump function in cardiac myocytes. *Circ Res*. 2006;99(12):1376–1383.
21. Hüser J, Lipsius SL, Blatter LA. Calcium gradients during excitation-contraction coupling in cat atrial myocytes. *J Physiol*. 1996;494(pt 3):641–651.
22. Berlin JR. Spatiotemporal changes of Ca^{2+} during electrically evoked contractions in atrial ventricular cells. *Am J Physiol*. 1995;269(3 pt 2):H1165–H1170.
23. Michailova A, DelPrincipe F, Egger M, Niggli E. Spatiotemporal features of Ca^{2+} buffering diffusion in atrial cardiac myocytes with inhibited sarcoplasmic reticulum. *Biophys J*. 2002;83(6):3134–3151.
24. Trafford AW, Díaz ME, Eisner DA. A novel, rapid and reversible method to measure Ca buffering and time-course of total sarcoplasmic reticulum Ca content in cardiac ventricular myocytes. *Pflugers Arch*. 1999;437(3):501–503.
25. Solaro RJ. Modulation of cardiac myofilament activity by protein phosphorylation. In: Page E, Fozzard H, Solaro RJ, eds. *Handbook of Physiology*. New York, New York, USA: Oxford University Press; 2001:264–300.
26. Pi Y, Zhang D, Kemnitz KR, Wang H, Walker JW. Protein kinase C and A sites on troponin I regulate myofilament Ca^{2+} sensitivity ATPase activity in the mouse myocardium. *J Physiol*. 2003; 552(pt 3):845–857.
27. Schober T. et al. Myofilament Ca sensitization increases cytosolic Ca binding affinity, alters intracellular Ca homeostasis, and causes pause-dependent Ca-triggered arrhythmia. *Circ Res*. 2012;111(2):170–179.
28. Izu LT, Means SA, Shadid JN, Chen-Izu Y, Balke CW. Interplay of ryanodine receptor distribution and calcium dynamics. *Biophys J*. 2006;91(1):95–112.
29. Sheehan KA, Zima AV, Blatter LA. Regional differences in spontaneous Ca^{2+} spark activity regulation in cat atrial myocytes. *J Physiol*. 2006;572(pt 3):799–809.
30. Woo SH, Cleemann L, Morad M. Spatiotemporal characteristics of junctional and nonjunctional focal Ca^{2+} release in rat atrial myocytes. *Circ Res*. 2003;92(1):e1–e11.
31. Williams GS, Chikando AC, Tuan HT, Sobie EA, Lederer WJ, Jafri MS. Dynamics of calcium sparks and calcium leak in the heart. *Biophys J*. 2011;101(6):1287–1296.
32. Forbes MS, Van Niel EE, Purdy-Ramos SI. The atrial myocardial cells of mouse heart: a structural and stereological study. *J Struct Biol*. 1990;103(3):266–279.
33. Richards MA, et al. Transverse (t-) tubules are a common feature in large mammalian atrial myocytes including human. *Am J Physiol Heart Circ Physiol*. 2011;301(5):H1996–H2005.
34. Dibb KM, et al. Characterization of an extensive transverse tubular network in sheep atrial myocytes and its depletion in heart failure. *Circ Heart Fail*. 2009;2(5):482–489.
35. Bers DM. *Excitation-Contraction Coupling and Cardiac Contractile Force*. Dordrecht, the Netherlands: Kluwer Academic Publishers; 2001.
36. Cheng H, Lederer WJ. Calcium sparks. *Physiol Rev*. 2008;88(4):1491–1545.
37. Sheehan KA, Blatter LA. Regulation of junctional and non-junctional sarcoplasmic reticulum calcium release in excitation-contraction coupling in cat atrial myocytes. *J Physiol*. 2003; 546(pt 1):119–135.
38. Belus A, et al. Effects of chronic atrial fibrillation on active and passive force generation in human atrial myofibrils. *Circ Res*. 2010;107(1):144–152.
39. Hove-Madsen L, et al. Atrial fibrillation is associated with increased spontaneous calcium release from the sarcoplasmic reticulum in human atrial myocytes. *Circulation*. 2004;110(11):1358–1363.
40. El-Armouche A, et al. Molecular determinants of altered Ca2+ handling in human chronic atrial fibrillation. *Circulation*. 2006;114(7):670–680.
41. Greiser M, et al. Distinct contractile and molecular differences between two goat models of atrial dysfunction: AV block-induced atrial dilatation and atrial fibrillation. *J Mol Cell Cardiol*. 2009;46(3):385–394.
42. Heijman J, Dewenter M, El-Armouche A, Dobrev D. Function and regulation of serine/threonine phosphatases in the healthy and diseased heart. *J Mol Cell Cardiol*. 2013;64:90–98.
43. Hatem SN, et al. Different compartments of sarcoplasmic reticulum participate in the excitation-contraction coupling process in human atrial myocytes. *Circ Res*. 1997;80(3):345–353.
44. Bers DM. Cardiac ryanodine receptor phosphorylation: target sites and functional consequences. *Biochem J*. 2006;396(1):e1–e3.
45. Despa S, Bers DM. Na^+ transport in the normal and failing heart — remember the balance. *J Mol Cell Cardiol*. 2013;61:2–10.
46. Ottolia M, Torres N, Bridge JH, Philipson KD, Goldhaber JI. Na/Ca exchange and contraction of the heart. *J Mol Cell Cardiol*. 2013;61:28–33.
47. Despa S, Kockskämper J, Blatter LA, Bers DM. Na/K pump-induced [Na](i) gradients in rat ventricular myocytes measured with two-photon microscopy. *Biophys J*. 2004;87(2):1360–1368.
48. Sossalla S, et al. Altered Na(+) currents in atrial fibrillation effects of ranolazine on arrhythmias and contractility in human atrial myocardium. *J Am Coll Cardiol*. 2010;55(21):2330–2342.
49. Christ T, et al. Arrhythmias, elicited by catecholamines and serotonin, vanish in human chronic atrial fibrillation. *Proc Natl Acad Sci U S A*. 2014;111(30):11193–11198.